IAHR AIRH

25th IAHR International Symposium on Ice
Trondheim, 23 - 25 November 2020

Static ice loads on a dam in a small Norwegian reservoir

Chris Petrich[1], Irina Sæther[1], Megan O'Sadnick[1,2], Bård Arntsen[1]
[1] SINTEF Narvik, Narvik, Norway
[2] UiT The Arctic University of Norway, Tromsø, Norway
christian.petrich@sintef.no

Ice loads on a concrete dam have been calculated from stress measurements in Taraldsvikfossen Reservoir, a small reservoir in Narvik, Norway, during three winter seasons. Ice thickness was in the range of 0.5 to 1.0 m, and both thermal ice loads were observed and water level fluctuations up to 30 cm were observed when the ice cover froze to the spillway. The maximum global line load measured was 60 to 90 kN/m, in line with current design guidelines in Norway. Consistent with earlier reports, line loads were not evenly distributed along the dam face. A thermal line load model was able to reproduce the approximate shape and magnitude of many line load peaks even when the measured vertical stress profile could not be reproduced by the model. The results add to an extremely small body of data in Norway and motivate investigations in other parts of the country with expected higher or lower ice loads.

1. Introduction

Static ice loads form a significant contribution to the design load of dams of low height in cold climates. They have been attributed to thermal expansion of an ice cover during warm spells and refrozen fractures in the presence of water level fluctuations (e.g. Comfort et al., 2003; Stander, 2006; Petrich et al., 2015; O'Sadnick et al., 2016a). Design standards are based on empirical measurements as current understanding of the magnitude of ice loads is still limited (Comfort et al., 2003; Gebre et al., 2013; Timco et al., 1996). In Norway, static ice loads between 100 and 150 kN/m are generally assumed (NVE, 2003).

The only ice load measurements performed within Norway are those of Hoseth and Fransson (1999) at Silvatnet near Narvik, and the campaigns at Taraldsvikfossen Reservoir in Narvik, some of which form the basis of this study (Petrich et al. 2014, 2015; O'Sadnick et al., 2016a). All measurements targeted thermal ice loads and were performed in reservoirs with nominally constant water level. Hoseth and Fransson (1999) deployed three stress cells in front of a dam, rotated 120° with respect to each other 0.2 m below the ice surface. They derived line loads of up to 135 kN/m in 0.5 to 0.6 m thick ice by assuming a linear stress profile through the ice. They also found that the shapes of the peaks could be reproduced by an ice stress model after Bergdahl (1978). In the present study line loads were calculated for three winter seasons from vertical stress profiles. Since the vertical stress profiles observed were generally not linear, similar to observations in independent studies (e.g. Morse et al., 2009), an uncertainty arises from the extrapolation of stresses above and below the cell arrangement. Measured line loads are compared with thermal line loads calculated from ice temperature measurements in order to assess whether they are of thermal or mechanical origin.

Taraldsvikfossen Reservoir is a small (3400 m^2) drinking water backup reservoir fed by a creek (Taraldsvikelva) at 213 m elevation, 68.436782° N, 17.498563° E. The crown of the dam is 0.5 m above the nominal water level which is maintained by a spillway. The typical ice thickness is between 0.5 and 1.0 m, and the ice is attached to the dam. Aspects of the reservoir and ice stresses during the three winters covered in this study were presented in more detail elsewhere (Petrich et al. 2014, 2015; O'Sadnick et al., 2016). It became clear in those studies that Taraldsvikfossen Reservoir exhibits at least two different sources of ice stresses: thermal stresses in response to ice temperature changes, and mechanical in response to small (decimeter) water level fluctuations that typically coincide with partial flooding of the ice surface. The latter arose from a creek discharging into the reservoir while the ice cover was frozen to the spillway. Creek discharge while the ice cover was frozen to the spillway resulted in visible upward movement of the ice cover away from the dam. This resulted in the formation of several decimeters of superimposed ice at the dam.

2. Methods

2.1 Ice Stresses

Ice stresses were measured with custom designed oil-filled GeoKon 4850 stress cells that measured internal temperature at the same vertical level as pressure (Petrich et al., 2015). The cells consisted of two rectangular steel plates (100 mm×200 mm) welded together around the periphery with de-aired oil occupying the space between the plates. A short tube connected the cell to a vibrating wire pressure transducer that also measured temperature with a temperature-dependent resistor (cf. cells sketched in Figure 1). Between one and three cameras mounted around the reservoir took timelapse imagery every 30 minutes. A water

pressure gauge had been installed at the dam at 1.3 m water depth in winter 2013/14. It froze in that winter but provided valuable data the following winter.

A limitation of the stress measurement method is that flatjacks cannot reliably measure tension because the ice may detach from the probes, or the oil inside the probes may start to boil in the presence of a vacuum. The latter problems may arise from approx. 100 kPa in tension. Hence, it is assumed in this study that measured line loads are systematically biased high in the presence of tensile stresses (cf. Section 3).
The configuration of stress cells differed between seasons. However, in each case there were both measurement stations that measured vertical profiles and measurement stations with only one cell. Only stations with multiple cells are used in this study, and those were located near the center of the dam. Cells that were frozen into the ice in 2012/13 and 2013/14 showed characteristic stresses during freeze-in (e.g., Fransson 1988), and data analysis stared after those freeze-in peaks had relaxed during warmer weather.

During winter 2012/13, stations were installed 1 m in front of the dam and in the middle of the reservoir, approx. 10 m from dam (cf. Petrich et al., 2015). At the time of measurement, ice thickness was approx. 0.85 m near the dam (Stations 3 and 5) and 1.0 m at Station W. During winter 2013/14, the first half of each station was installed at the dam early in the season and the second half in the ice 2 m in front of the dam in February. These were intended for inter-comparison but are interpreted as single stations here due to unexpected, excessive superimposed ice formation at the dam (Figure 2). During winter 2014/15, cells were installed at the dam with one cell placed above the water line to account for anticipated superimposed ice formation. As a result, only a comparatively small amount of superimposed ice formed above the upper-most cell (Figure 3).

Line loads were calculated as a lower and nominally upper bound. For lower bound calculations, each stress measurement was multiplied by the vertical separation of the stress cells, i.e. 0.15 m in all seasons (exception: 0.25 m at Station W in 2012/13), and the results were summed. However, due to the peculiar cell configuration in winter 2013/14, the lower-most cell 2 m in front of the dam was averaged with the upper-most cell at the dam (cf. Figure 2).

Simple stress extrapolations were performed to estimate nominally upper bound line loads, i.e., to account for ice above and below the stress cells. In season 2012/13 the depth weights of the upper and lower most cells at each station were changed to 0.25, and 0.35 m, respectively (0.275 and 0.45, respectively at Station W), in season 2013/14 they were 0.25 and 0.25 m, respectively, and in season 2014/15 they were 0.3 and 0.15 m, respectively. There was insufficient linearity in the stress profiles to justify a linear extrapolation.

Usually, loads to not act homogeneously along the dam which implies that the average load experienced by a section of the dam will be less than the peak load (e.g., Côté et al., 2016). Hence, a global line load was calculated as the average of the line loads of all stations at a given time (local line loads) to quantify the magnitude of the influence of dam design.

2.2 Thermal Modeling

Modeling of thermal ice loads assumes knowledge of ice thickness and temperature in addition to (implicit) assumptions about properties of ice and dam. While ice growth and temperatures are reasonably straight-forward to model (e.g., Bergdahl 1978; Petrich and Arntsen, 2018), measurements are used in this study since they are available. Temperature

measurements at the stress cells have been used since the temperature sensors were at the same vertical position in the ice as the center of the respective stress cell.

Ice stresses are modeled as a linear spring in series with a non-linear dashpod (Bergdahl, 1978). Like Petrich and Arntsen (2018), we used the equation and coefficients derived for "Cell 4" in Petrich et al. (2015). This particular sensor is not used in the present study, i.e. the model is not fitted to data presented in this study, although it is based on measurements in the same reservoir (i.e. Taraldsvikfossen Reservoir, winter 2012/13).

Line loads were calculated by integrating the vertical thermal stress distribution normal to the dam through the thickness of the ice (Bergdahl, 1978; Petrich and Arntsen, 2018). Following earlier work (Bergdahl, 1978; Cox, 1984; Fransson 1988; Petrich et al., 2015), the thermal stress at a particular vertical position in the ice was calculated as

$$\frac{d\sigma}{dt} = A\frac{dT}{dt} - B\left(\frac{T_0}{\bar{T}}\right)^m \left(\frac{\sigma}{\sigma_0}\right)^n \qquad [1]$$

where the stress σ is positive in compression (extension to negative stresses as in Petrich et al., 2015), dT/dt is the rate of temperature change and $\bar{T}$ is the temperature in °C at the same vertical level as the stress, T_0 = -1 °C and σ_0 = 100 kPa are scale constants, m=1.92 from Cox (1984), and A=200 kPa/K, B=342 kPa/day, and n=3.7 are parameters of Cell 4 from Petrich et al. (2015). The stress was fixed at 0 whenever $T \geq 0$ °C. Equation 1 was solved implicitly in time. Equation 1 does not account explicitly for elasticity of the dam or the movement of the dam in response to temperature changes.

Unlike earlier work, modeled stresses were capped at 30 kPa in tension to approximate measurement limitations of flat jacks (c.f. Section 2.1), i.e. if a modeled tensile stress exceeded this value at the end of a time step it was set to 30 kPa. For the purpose of this study, the impact of this cap on model results is largely cosmetic given the accuracy sought: it improves agreement with measurements of low ice loads dramatically while increasing some modeled peak thermal loads (by <40 kN/m). Note that this cap was not used to obtain the coefficients in Equation 1 (Petrich et al., 2015).

Thermal stresses were calculated from the temperature measurements within each stress cell and integrated using the approach for lower bound line loads described in Section 2.1. A limitation of this approach is that temperatures measured at the stress cells are not necessarily representative of the temperatures in most of the ice cover. For example, cells located at the dam may be affected by heat conduction through the dam, insulation form snow drifts caught by the dam, and may experience an unrepresentative thermal regime during partial flooding of the reservoir ice surface. Another limitation of the present approach is that no account was taken for any difference in ice physical properties with depth even though superimposed ice due to surface flooding, snow-ice, and congelation ice may have been present at the same time.

3. Results and Discussion

Measurements and thermal model results are compared for three seasons in Figures 4, 5, and 6, respectively. Measured ice thickness profiles perpendicular to the dam are shown in Figure 3. While no significant ice loads were registered anymore in winter 2014/15 after the profile in Figure 3 had been measured (phase 8), the profile serves to illustrate an actual thickening of ice close to the dam. The gap layer in the ice cover >5 m in front of the dam would have

fixed the bulk of the ice at 0 °C, explaining the absence notable loads in spite of air and ice temperature variations at the dam.

3.1 Winter 2012/13

Figure 4 shows line load data of two stations mounted 2 m in front of the dam (Stations 3 and 5, Figure 4b and c, respectively), and one station mounted 10 m in front of the dam (Station W, Figure 4d). Ice thickness 1 m in front of the dam was 0.75 m on 9 February (0.3 m freeboard at the sites of deployment due to ice formation from surface flooding at the end of December).

Freeze-in artifacts lasted from probe deployment until a week-long warm spell at the end of February. The ice cover remained detached from the spill way following the warm spell and there were no further indications of water level fluctuations in the timelapse imagery or otherwise until break-up. After the warm spell, phase 1 started with a load event that, counter-intuitively, corresponded to a 10 °C drop in air temperature, followed by small load variations (Figure 4). The thermal model reacted on the initial decrease in air and ice temperature by predicting a negative load, i.e. ice pulling the dam, modulated by temperature fluctuations that correlate positively with the load variations at Stations 3 and 5, and negatively with loads calculated for Station W 10 m away from the dam. Phase 2 is characterized by five consecutive load events that are reasonably well reproduced by the thermal load model. Following an abrupt decrease in temperature, the thermal model and observations show fluctuations between tension and compression loads in phase 3. Like in phase 1, measured line load variations correlated positively with modeled loads at Stations 3 and 5, and negatively at Station W. The week-long load period of phase 4 and subsequent smaller variations in line load are reproduced reasonably well by the thermal load model. The ice decayed during phase 5 when no more load events were recorded or modeled.

There is a phase lag in the temperature data and stress signal from the top-most to the bottom-most stress cell as one would expect in the presence of vertical heat conduction through the ice (Figure 7).

With the exception of the initial peak in phase 1, the peak local line loads were between 60 and 90 kN/m, depending on how stresses are extrapolated. The nature of the initial peak in phase 1 is not clear. However, since they are entirely due to high stresses at the top-most cells they could potentially be a form of freeze-in artifacts. Peak global line loads (Figure 4e) were lower than local loads, i.e. 40 to 80 kN/m, depending on extrapolation.

3.2 Winter 2013/14

Figure 5 shows line load data of three stations that combine stress cells at the dam with stress cells in the ice. The period shown starts following the freeze-in period of the ice-borne sensors and ends prior to melt-out artifacts of the dam-borne sensors (i.e., dam-borne sensors were torn out of anchorage). No vertical movement was visible in the timelapse camera sequences since 4 February 2014. There was 50 cm superimposed ice at the dam since January, and ice thickness was 0.75 m during deployment on 11 February.

Three major load events (phases 1, 3, 7) appear to have been thermal loads based on their agreement with the thermal model. However, there is a small discrepancy in either time or magnitude between measurements and thermal model in phase 1. At this point we cannot assess whether this is a phenomenon that merits further investigation. Phases 2, 4, and 6 are marked by only small measured and modeled loads. In fact, the ice was flooded during phase

4 and all stress cells read 0.0 °C by the end of the phase. Line load peaks during phase 5 do not correlate with the thermal model and end suddenly, possibly due to some global rearrangement of the ice cover.

Ice temperature data show air temperature signals propagating downward compatible with vertical thermal conduction. However, unlike winter 2012/13, this pattern is not reflected in the stresses registered by the respective cells (Figure 8). Instead, stresses increased either more-or-less simultaneously (phase 7), or in non-intuitive order (e.g. phase 3, Station D: starting at both top and bottom-most and ending in the center). Hence, while the model performed reasonably well in predicting the over-all line load, it performed poorly at predicting stresses at individual cells.

Global thermal line loads reached close to 100 kN/m on three occasions this season with a measured maximum at 110 to 130 kN/m. However, loads derived this season are questionable in the light of the unconventional stress cell configuration.

3.3 Winter 2014/15

Ice stresses were recorded only at the dam and no freeze-in or break-up artifacts were observed. Only the most interesting part of the season is shown in Figure 6 as ice loads early and late in the season were low. Figure 6a shows water pressure data converted to water column equivalent in addition to air temperature. Ice thickness was 0.4 m on 5 January. On 5 February it was 0.8 to 0.9 m at the dam, reducing to 0.6 m 5 to 10 m in front of the dam. The sensors installed above nominal water level were exposed on 5 Jan but covered in ice by 22 January (Figure 9). Superimposed ice thickness at the dam was 0.25 m on 4 February.

Phases 1, 3, 5, and 6 had significant excursions of the water column equivalent (Figure 6a). Each excursion was readily visible in the site camera timelapses. Further confirmation was obtained as a result of a misunderstanding that led to holes being drilled in the ice cover close to the dam approximately 2 hours before the peak water level in phase 6. All holes had negative freeboard, i.e. they flooded the surface, with one hole creating a 0.1 m high water sprout.

Ice loads were small during phases 2 and 8 in spite of significant ice temperature changes that are reflected in the modeled thermal line loads. The absence of loads in phase 2 could be explained by assuming mechanical failure of the ice cover during phase 1. Measurements of the peaks during phases 4 and 7 are generally compatible with the thermal load model. The peak in phase 4 was lower than modeled, possibly because the water level was decreasing back to normal level at the same time. The shoulder in phase 7 appears to correlate well with the model.

In phase 6, the onset of the measured load peak appeared as the water level increased and before air or ice temperatures rose and had therefore been missed by the thermal model in Station C (Figure 6c). However, measured loads at Stations B and D only started to increase after air temperatures rose. The thermal model is catching up with the measurements toward the end of phase 6, presumably as a result of ice temperature increase from surface flooding. The initial peak appears to be related to water level increase. A peak of similar origin appears in phase 5: the thermal model eventually catches up once the surface flooded around the time of maximum deflection. The peaks in phases 1 and 3 correlate likewise with an upward movement of the ice cover. However, camera images show that the ice surface started to flood from the creek toward the dam around the same time. This should have created a

thermal load. Since the flooding did not extend over the entire ice surface, no corresponding temperature signal was detected by the temperature sensors at any of the stations during phase 1, and at station D during phase 3 and hence those are not modeled as a thermal load (Figure 6b,c,d).

It is difficult to unambiguously distinguish loads due to waterlevel changes from thermal loads in phases 1, 3, 5, and 6 since water level changes were accompanied by partial flooding of the ice surface. The vertical stress profile that developed in the flooded areas could have averaged out in the regions that were not flooded closer to the dam where it got further modified by cracks and an upward-moving ice cover, removing the characteristic staggered stress development through depth that was observed in 2012/13. Similarly, the stress profiles during phases 4 and 7 do not show thermal characteristics (Figure 9) even though the aggregated local line loads do (Figure 6). Hence, the local line load may be a more robust measure of ice processes than the depth-resolved stress profile.

Peak line loads this season were related to inrush of water into the reservoir that caused upward-movement and partial flooding of the ice surface. Separating the contributions of the two mechanisms is not trivial.

The registered local peak line load was 170 to 240 kN/m at Station C, phase 6, just before readings at two stress cells exceeded 50 kPa in tension. The global line loads were 60 to 90 kN/m at this point.

4. Conclusion

Local line loads have been calculated for three years of ice stress measurements at Taraldsvikfossen Reservoir near Narvik. While the reservoir had nominally no waterlevel varions in winter it did show significant excursions while the ice cover was frozen to the spillway.

It was found that local line loads may follow development predicted by the thermal load model even when individual stress measurements within the corresponding profiles do not (2013/14 and 2014/15). It was hypothesized that this is related to inhomogeneous ice temperature profiles across the reservoir (in particular, local flooding) and cracks in the ice.

The maximum global line load registered was 60 to 90 kN/m with a local maximum of 170 to 240 kN/m. The ranges result from uncertainty because the measured vertical stress profiles did not extend through the entire depth of the ice and the stress profiles generally did not suggest linearity. The assessment excludes periods where at least one stress cell recorded tensile stresses >50 kPa due to systematic limitations of the method to measure tension. Season 2013/14 had been excluded from this assessment due to additional uncertainties that stem from the stress cell configuration. However, global line loads were probably in the same range. Since the maximum line load experienced by a section of the dam decreases with increasing width of the construction sections (e.g., Côté et al., 2016), the dam-dependent relevant peak line load should lie between local and global loads.

Rarely discussed aspects of the measurements include the observation of negative line loads, i.e. ice pulling the dam, and the implicit assumption that the dam is a rigid body that does not move in response to thermal or mechanical forces. The latter could potentially introduce dam-dependence of line load measurements.

Acknowledgments
This work was supported by the Research Council of Norway NORDSATSING program, grant number 195153 (ColdTech) and industry partners, by Statkraft and by the Norwegian Water Resources and Energy Directorate (NVE).

References
Côté, A., A. Taras, G. Comfort, and B. Morse, 2016. Static ice loads at dam face and at far field. In Proceedings of the 23rd IAHR International Symposium on Ice, Ann Arbor, MI, USA, 31 May–3 June 2016, 8 pp.

Cox, G. F. N., 1984. A preliminary investigation of thermal ice pressures. Cold Regions Science and Technology, 9, 221–229.

Fransson, L., 1988. Thermal ice pressure on structures in ice covers. Doctoral Thesis, Luleå University of Technology, Sweden, 161 pp.

Gebre, S., Alfredsen, K., Lia, L., Stickler, M., Tesaker, E., 2013. Review of ice effects on hydropower systems. Journal of Cold Regions Engineering 27 (4), 196–222.

Hoseth, K.A., Fransson, L., 1999. Istrykk på dammer, Måleprogram dam Silvann, vinter 98–99. Report 22/1999. Norwegian Water Resources and Energy Directorate (NVE), Oslo, 34 pp.

Morse, B., E. Stander, A. Coté, J. Morse, P. Beaulieu, A. Tarras, P. Noël, and Y. Pratt, 2009. Ice interactions at a dam face. In Proceedings of the 15th Workshop on River Ice, St. John's, Canada, June 2009, 11 pp.

NVE, 2003. Retningslinje for Laster og Dimensjonering til §§ 4–1 og 4–2 i Forskrift om Sikkerhet og Tilsyn med Vassdragsanlegg Norges Vassdrags- og Energidirektorat. Norwegian Water Resources and Energy Directorate (NVE), Oslo, Norway, 25 pp.

O'Sadnick, M., C. Petrich, B. Arntsen, and B. Sand, 2016. Observations of Ice Stress at Taraldsvikfossen Reservoir, Narvik, Norway. In Proceedings of the 23rd IAHR International Symposium on Ice, Ann Arbor, Michigan, USA, 31 May to 3 June 2016. 8 pp.

Petrich, C., I. Sæther, L. Fransson, B. Sand, and B. Arntsen, 2014. Preliminary results from two years of ice stress measurements in a small reservoir, In Proceedings of the 22nd IAHR International Symposium on Ice, Singapore, 11–15 August 2014, A. W.-K. Law (ed), NEWRI Nanyang Technological University, Singapore. 452-459.

Petrich, C., I. Sæther, L. Fransson, B. Sand, and B. Arntsen, 2015. Time-dependent spatial distribution of thermal stresses in the ice cover of a small reservoir. Cold Regions Science and Technology, 120, 35-44, https://dx.doi.org/10.1016/j.coldregions.2015.09.003.

Petrich, C., and B. Arntsen, 2018. An overview of trends and regional distribution of thermal ice loads on dams in Norway. In Proceedings of the 26th International Congress of the International Commission of Large Dams (ICOLD), Q.101, R.72, Vienna, Austria, 1-7 July 2018, 1210-1224.

Stander, E., 2006. Ice stresses in reservoirs: Effect of water level fluctuations. Journal of Cold Regions Engineering, 20(2), 52-67.

Timco, G.W., Watson, D.A., Comfort, G.A., Abdelnour, R., 1996. A comparison of methods for predicting thermally-induced ice loads. Proceedings of the 13th IAHR Symposium on Ice, Beijing, China. vol. 1, pp. 241–248.

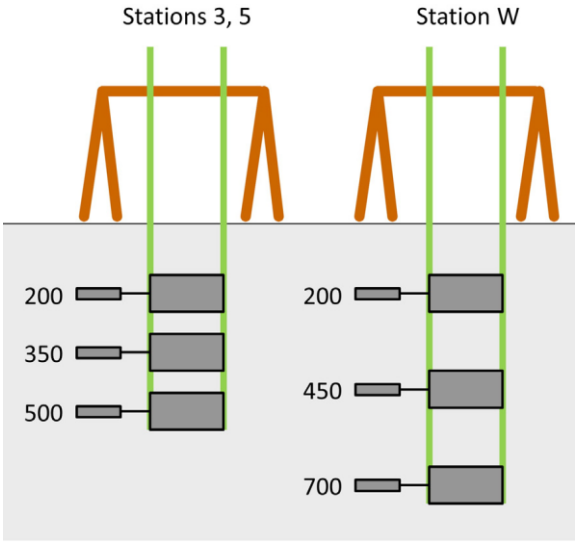

Figure 1. Sketch of the vertical positions of stress cells in winter 2012/13. Numbers indicate distance to the ice surface in mm at the time of depoyment. Stations 3 and 5, and Station W were placed 1 m and 10 m in front of the dam, respectively.

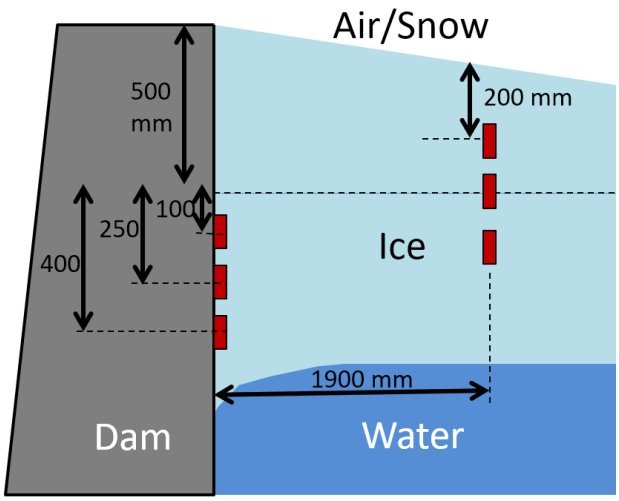

Figure 2. Sketch of the vertical positions of stress cells in winter 2013/14. The dashed horizontal line indicates the water level (i.e., approx. ice level) at the time of deployment of the dam-borne sensors. Sketch is not to scale.

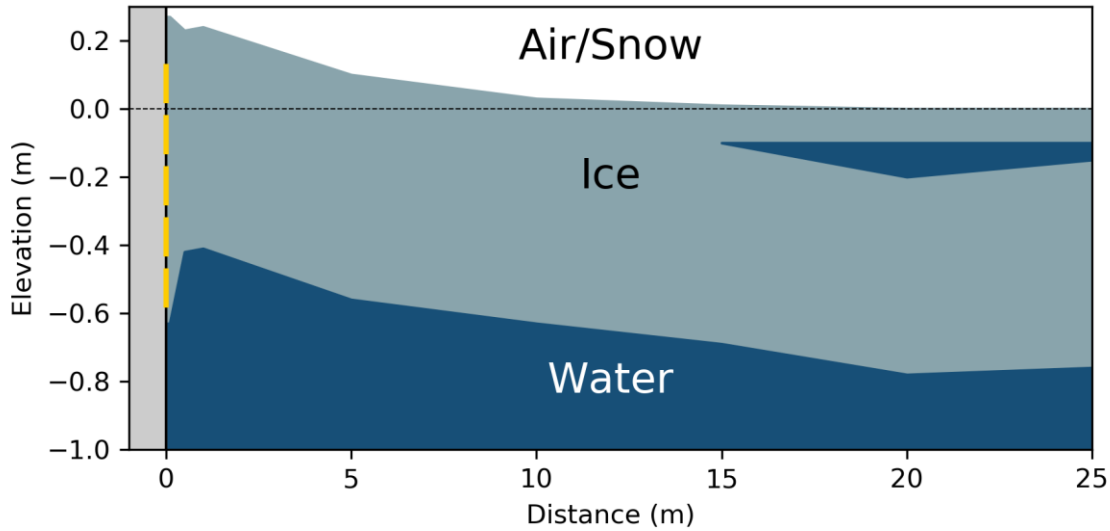

Figure 3. Measured vertical ice profile along a transect normal the dam (distance 0 m) on 6 March 2015 (phase 8), i.e. several weeks after significant load signals had been recorded. Positions of the stress cells at the dam during winter 2014/15 are marked (yellow lines at distance 0 m). 0 m elevation is the waterline at the time of measurement. Note the gap layer in the ice from 15 m onwards.

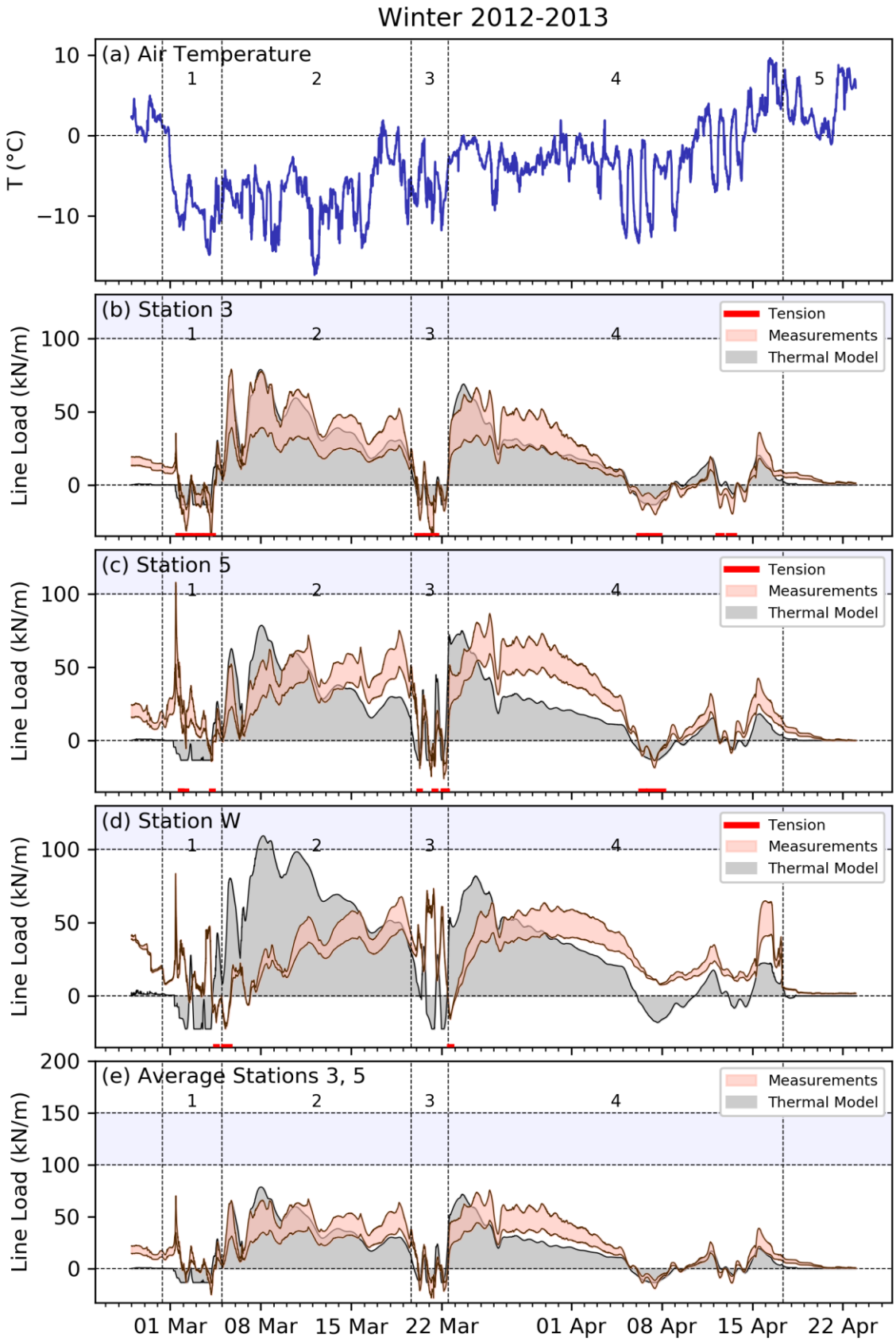

Figure 4. (a) Air temperature, (b,c) ice loads in winter 2012/13 measured and modeled at two stations, and (d) averaged loads. Red lines in (b) and (c) indicate that tensile stresses >50 kPa were measured.

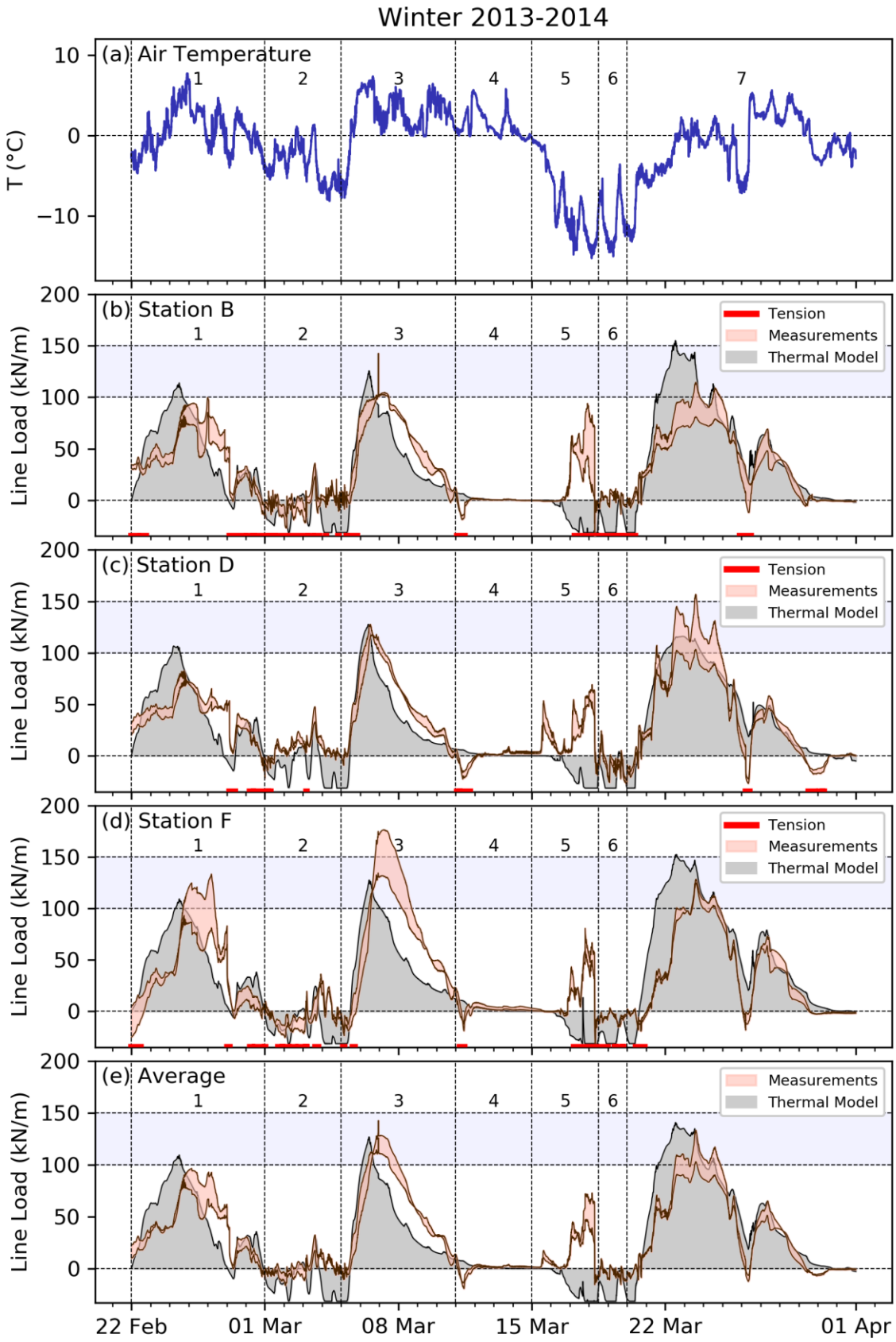

Figure 5. (a) Air temperature, (b,c,d) ice loads in winter 2013/14 measured and modeled at three stations, and (e) averaged loads. Red lines in (b), (c), and (d) indicate that tensile stresses >50 kPa were measured.

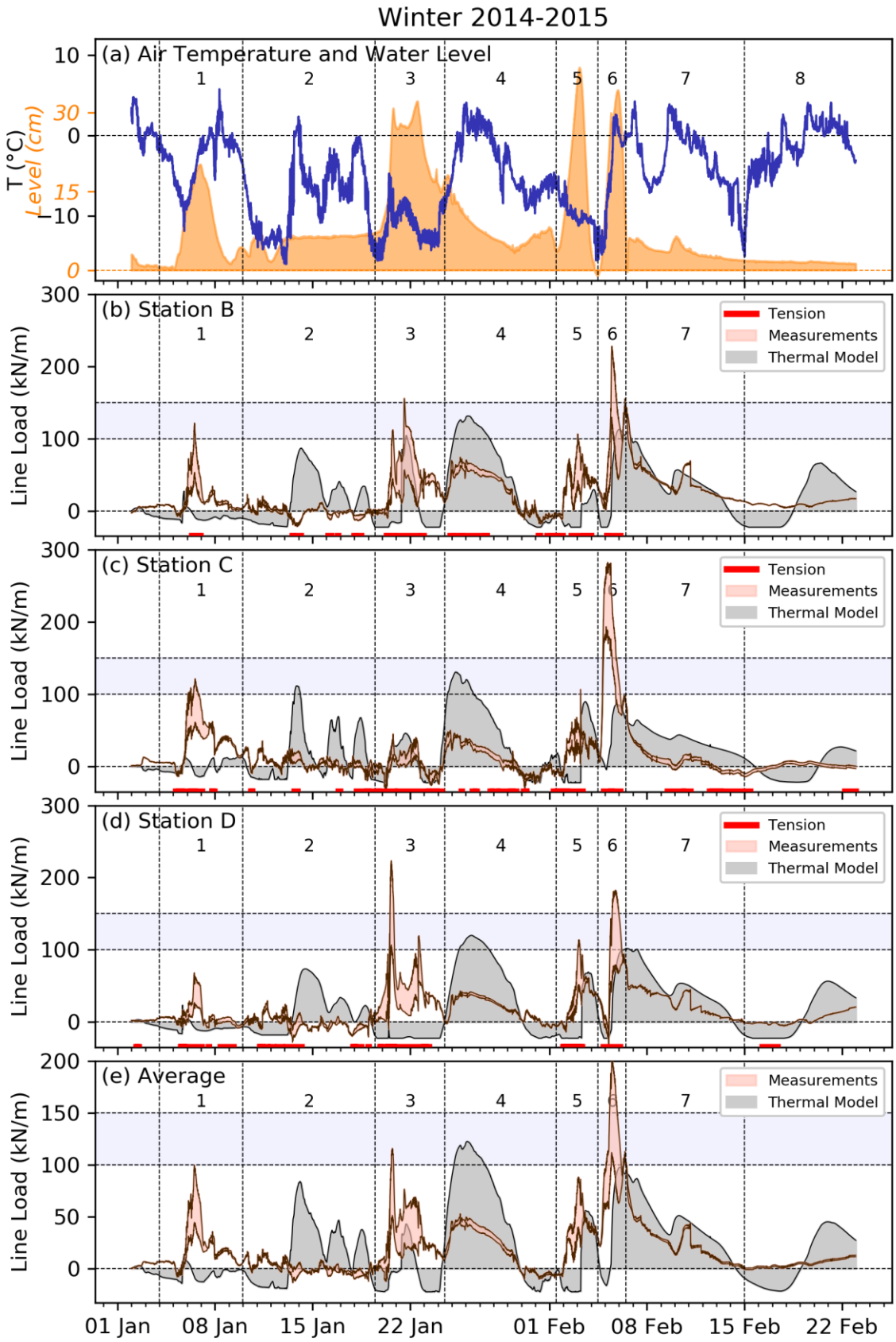

Figure 6. (a) Air temperature and water level, (b,c,d) ice loads in winter 2014/15 measured and modeled at three stations, and (e) averaged loads. Red lines in (b), (c), and (d) indicate that tensile stresses >50 kPa were measured.

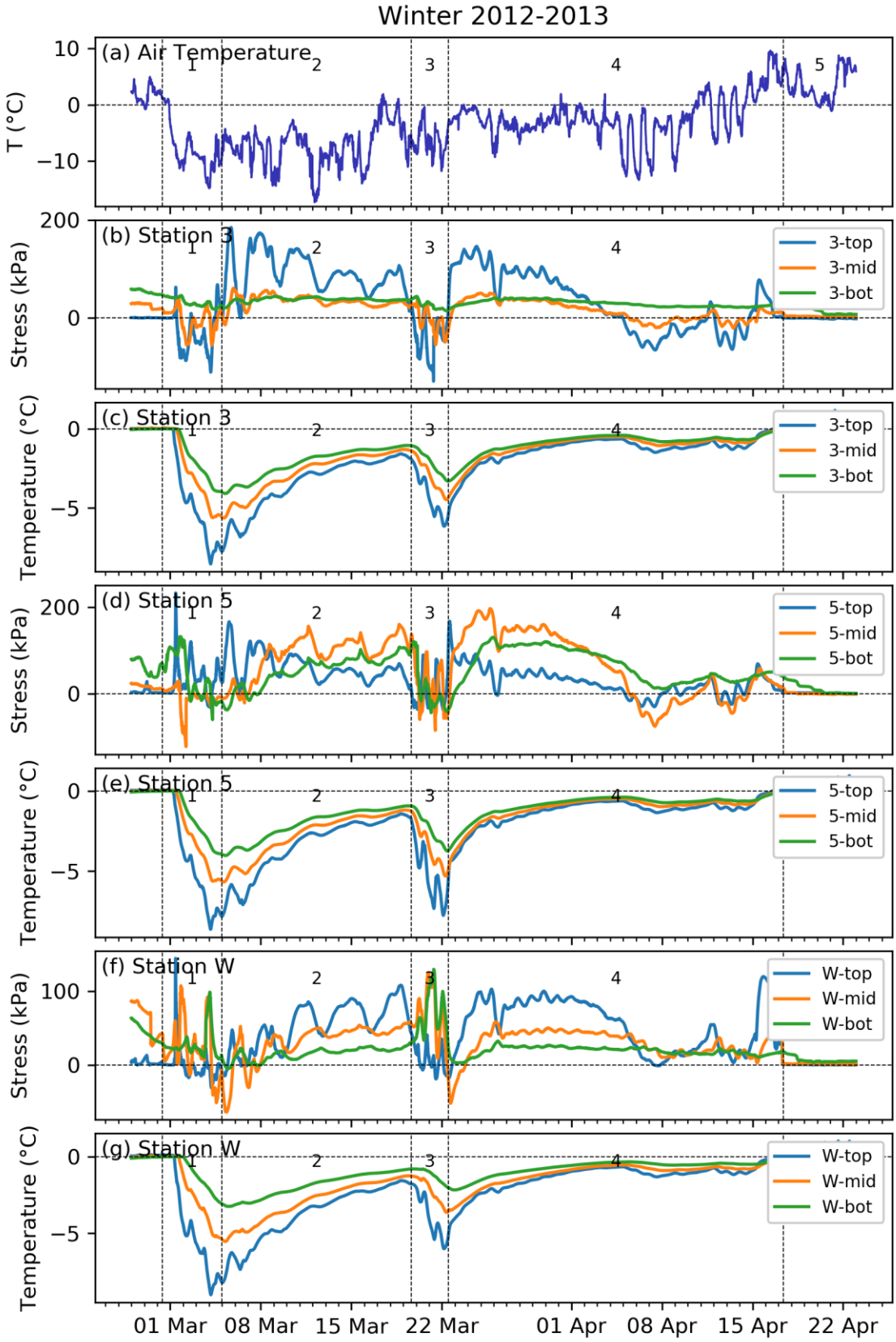

Figure 7. (a) Air temperature, (b,d,f) stresses positive in compression, and (c,e,g) ice temperatures measured in 2012/13. Cells are labeled top to bottom "top", "mid", "bot", respectively.

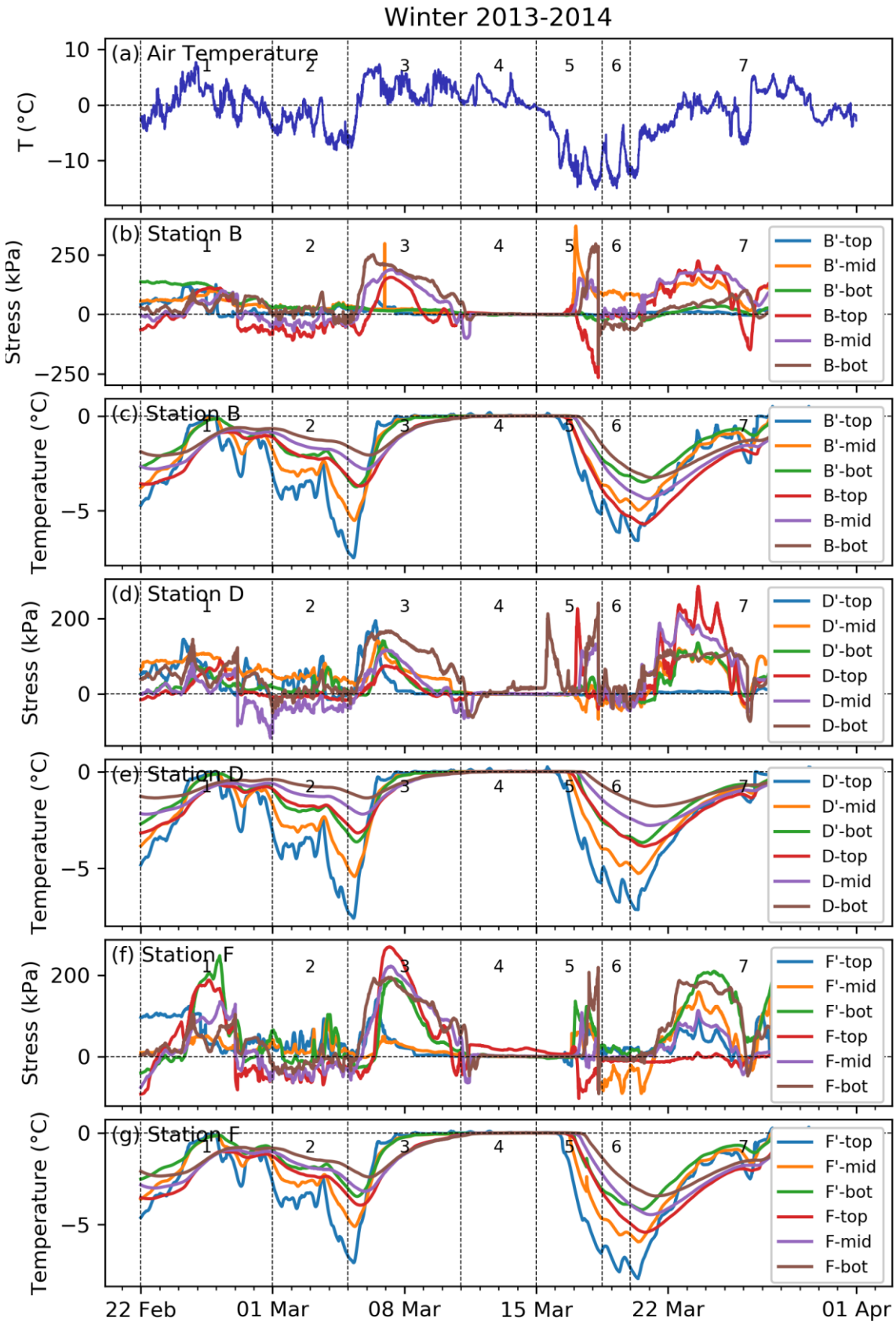

Figure 8. (a) Air temperature, (b,d,f) stresses positive in compression, and (c,e,g) ice temperatures measured in 2013/14. Cells are labeled top to bottom "top", "mid", "bot", respectively, with primed and unprimed cells in the ice and at the dam, respectively.

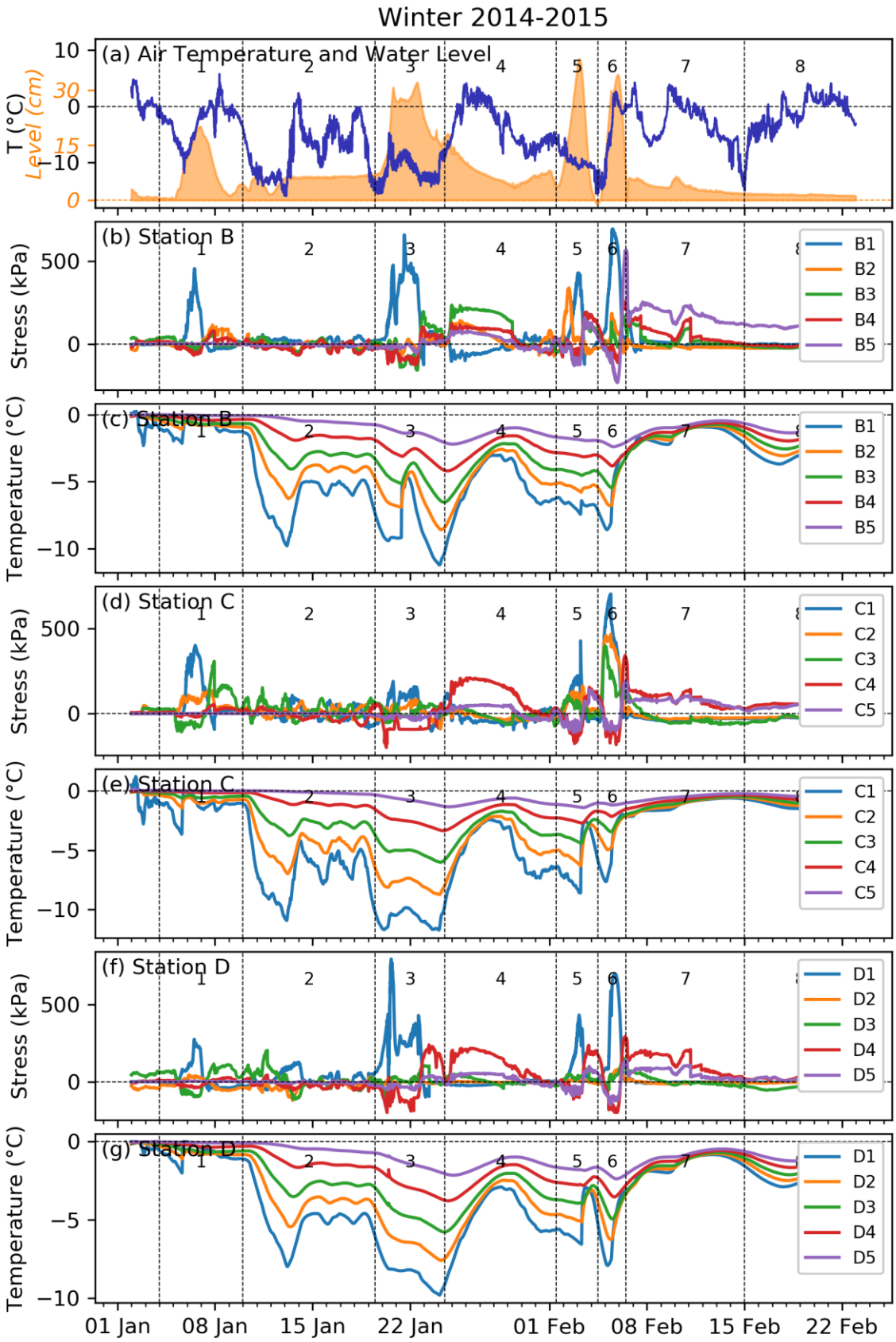

Figure 9. (a) Air temperature and water level, (b,d,f) stresses positive in compression, and (c,e,g) ice temperatures measured in 2014/15. Cells are labeled top to bottom from 1 to 5 where cell 1 had been installed above the nominal water line.